Interactive Segmentation of Media-Adventitia Border in IVUS

Jonathan-Lee Jones[1], Ehab Essa[1], Xianghua Xie[1,⋆], and Dave Smith[2]

[1] Department of Computer Science, Swansea University, UK
[2] ABM-UHT Morriston Hospital, Swansea, UK
http://csvision.swan.ac.uk/

Abstract. In this paper, we present an approach for user assisted segmentation of media-adventitia border in IVUS images. This interactive segmentation is performed by a combination of point based soft constraint on object boundary and stroke based regional constraint. The edge based boundary constraint is imposed through searching the shortest path in a three-dimensional graph, derived from a multi-layer image representation. The user points act as attraction points and are treated as soft constraints, rather than hard constraints that the segmented boundary has to pass through the user specified points. User can also use strokes to specify foreground (region of interest). The probabilities of region of interest for each pixel are then calculated and their discontinuity is used to indicate object boundary. This combined approach is formulated as an energy minimization problem that is solved using a shortest path search algorithm. We show that this combined approach allows efficient and effective interactive segmentation, which is demonstrated through identifying media-adventitia border in IVUS images where image artifact, such as acoustic shadow and calcification, are common place. Both qualitative and quantitative analysis are provided based on manual labeled datasets.

Keywords: Image segmentation, graph segmentation, Dijkstra shortest path, IVUS segmentation, media-adventitia border.

1 Introduction

The Intra-Vascular UltraSound (IVUS) imaging technique is a common-place catheter based technology, frequently used in cardiology diagnosis. This catheter based approach is widely used to assess the severity of any stenosis present and to categorize their morphology. It also allows for the measurement of vessel diameter the location of any lesions, as well as many other clinical and therapeutic studies [1]. In most IVUS images, a cross-section of the arterial wall is proceeded, with three regions: the lumen, the vessel (made up of the intima and media layers), and the adventitia surrounding the vessel wall. The media-adventitia border is the dividing layer representing the outer arterial wall. In IVUS images, the media

⋆ Corresponding Author.

R. Wilson et al. (Eds.): CAIP 2013, Part II, LNCS 8048, pp. 466–474, 2013.

can be seen as a dark band, with no other distinct features. It is encapsulated by the adventitia, which is a wide layer of fibrous connective tissue. Figure 1 provides an example of IVUS images.

There have been many different approaches to the problem of segmenting IVUS images, e.g. [1–6]. These can be broadly categorized into fully automatic methods, or methods that allow user interactions. In [2] the authors used contour detection and tracing with smoothness constraint and circular dynamic programming optimization to segment lumen border. It assumes homogeneity of the lumen region and high contrast between lumen and artery wall. Katouzian *et al.* [3] applied complex brushlet transform and constructed magnitudes-phase histograms of coefficients that contain distinct peaks corresponding to lumen and non-lumen regions. The lumen region is then segmented based on K-means classification and a parametric deformable model. Homogeneity of the lumen region is critical to the success of the method. Methods based on region growing, e.g. [6], also suffers from such limitations, since artifacts and irregularities are very common in IVUS images. Particularly for media-adventitia border, the region inside the border is non-uniform as seen in Fig. 1. Calcification in arterial wall leads to acoustic shadowing and high reflectance, as well as catheter and guid wire occlusion and artifacts. Stent placed against internal wall also produces strong features and acoustic shadows that break homogeneity. Incorporating user prior knowledge into segmentation hence is often necessary and has been shown to be an effective approach. For instance, in [4] Ehab *et al.* incorporated a shape prior into graph cut construction to regularize segmentation of media-adventitia border. However, these approaches generally require significant amount of training data and model re-training is often necessary in order to adapt to new dataset. User initialization is an alternative approach to transfer expert knowledge into segmentation, e.g. [7–13]. However, most user interactions are limited to either boundary based landmark placement or strokes indicating foreground and background regions. in this work, we propose an approach to combine these two different types of user interactions, i.e. boudary based and region based, to segment media-adventitia border in IVUS. The user points, however, are treated as soft constraint, instead of hard constraint in most interactive segmentation methods. We show that this soft user constraint allows effective combination of boundary and region based features. The method is evaluated on an IVUS dataset with manually labelled "ground-truth" and compared against state-of-the-art techniques.

2 Proposed Method

The proposed method involves the user selecting a series of points on the image. These represent the start and the end point for the segmentation, and the user selected points act as the attraction points in the shortest path search which results in the segmentation. In order to enhance the image segmentation, the user can also select areas for foreground using strokes. An energy functional is then formulated based on the combination of the attraction force that is computed using distance transform and the discontinuity in foreground probability.

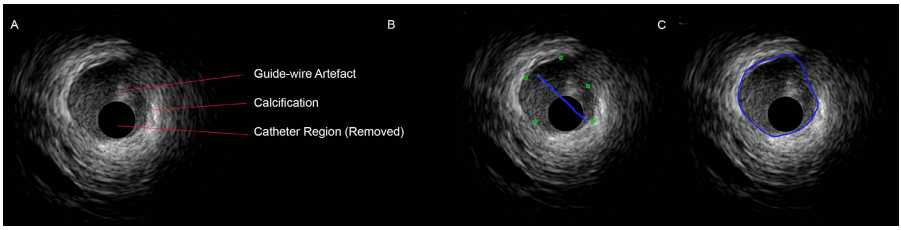

Fig. 1. (a) Original IVUS image. (b) User input (stroke to indicate region of interest and points to indicate boundary). (c) Segmentation result.

By assuming the user points are in a sequential order, we construct a multi-layer graph with each layer encapsulating a single individual user point. The segmentation problem is then transformed into searching the shortest path in this layered graph. This layered approach allows the segmentation to be carried out in polynomial time, instead of an NP-hard optimization problem, at the same time achieving global minima.

2.1 User Input

The proposed method allows two different types of user input: attraction points to indicate media-adventitia border and strokes to indicate region of interest. Fig. 1 provides an example of segmentation using the proposed method. Conventionally, user input to segmentation is focused on foreground and background specification [7–10]. For example, in [8], the user interaction consists of dragging a rectangle around the object of interest and in doing so the user specifies a region of background that is modeled in separating the foreground object. Several other methods require user to specify points on the object boundaries instead [11–13]. However, more often than not, these boundary based user points are treated as anchor points and the segmentation path has to go through them. This kind of hard constraint is not always desirable. It does not allow imprecise user input, and it can lead to difficulties in combining region based and boundary based approaches as discrepancy between different object descriptions is generally expected. Notably, in [13] the authors introduced soft constraint user point by embedding the user constraint in distance functions. The segmentation result is considered to be the shortest path to loosely connect the user points. However, it is known to be a NP-hard problem. Hence, it is assumed that the user points are placed in sequential order and such a constraint reduced the computational complexity to polynomial time. This user input constraint is generally acceptable in identifying IVUS media-adventitia borders. In this work, we follow this approach to treat boundary based user points. However, we also allow user to place region based strokes. These strokes are used to model foreground probability, and the discontinuity in foreground probability indicates the presence of object boundary. We combine these two types user input with image features in an energy functional which is then optimized using graph partitioning through finding the shortest path from the first to last user points.

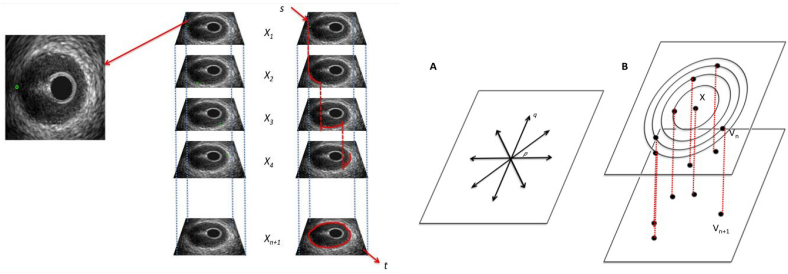

Fig. 2. Layered Graph Construction. The stack of images in the middle and right show how the graph is constructed out of a number of layers corresponding to the number of user points n. The diagrams on the right illustrate the internal layer edges (A) and the edges between neighboring layers (B).

2.2 Layered Graph Construction

In order to impose soft constraint for user point, we follow the approach proposed in [13] to construct a layered graph so that given a set of attraction points we fit a curve to follow the edges in the image and pass through the vicinity of the given points. The user points are assumed to be placed in a sequential order, which is acceptable in our application. The computational complexity, however, is reduced to polynomial time.

For each user point, $X_i, i \in \{1, 2, ..., n\}$, we create a layer of directed graph. In that way we have a series of layers equal to the number of user points n, plus an additional layer to ensure a closed curve, as shown in Fig. 2. This results in a multi-layer directed graph, $G = (V, E)$. For each pixel p, there exits an edge e to each of its neighboring 8 pixels on the same layer. Therefore, a pair of neighboring pixels $(p, q) \in N$ with a corresponding edge $e = (v_p, v_q)$ also have an edge to the corresponding point on the superseding layer $e = (v_{p_n}, v_{p_{n+1}})$. For each edge, we assign a weight w to build a weighted graph (G, w). These weights are calculated based on whether the edge is internal to a layer (w_i) or trans-layer (w_x). By creating the graph in this way, an order is established with the user points. Edges of zero weight are added from the start node r to each pixel in the first layer, and from the terminal node t to the last layer $n + 1$. If P is the set of pixels in the image, we can define the set of nodes V as $V = \{s, t\} \cup \{p \in P \wedge 1 \leq i \leq n + 1\}$ and thusly the set of edges as,

$$\begin{aligned} E = &\{(s, v_p) | p \in P\} \cup \{(v_p, n + 1h, t) | p \in P\} \\ &\cup \{(v_{p_i}, v\_q_i) | (p, q) \in N \wedge 1 \leq i \leq n + 1\} \\ &\cup \{v_{p_i}, v_{p_{i+1}}) | p \in P \wedge 1 \leq i \leq n + 1\} \end{aligned} \tag{1}$$

The segmentation is thus to find the shortest path from the start point r to the end point t, see Fig. 2.

2.3 Edge Weights and Energy Minimization

The edges on the directed layered graph are categorized as internal edges w_i within individual layers and interlayer edges w_x. The weighting for these two types edges is assigned differently.

The internal edges are assigned with two types of weights, i.e. boundary based edge weights and region based edge weights. The boundary based edge weights are calculated based on the magnitude of image gradients, i.e. using an edge detection function $g = 1/(1 + \nabla I)$ where I denotes the image or its smoothed version using, for instance, Gaussian. Hence, for any given edge between neighboring pixels (v_p, v_q) we assign a weight (w_e) according to $w_e((v_p, v_q)) := 1/2||p-q||(g(p) + g(q))$. The region based edge weights are computed from foreground probabilities. The user strokes placed in the foreground provide an estimation for foreground intensity distribution, which is then used to evaluate each pixel in the image. The discontinuity in this generated probability map is then used to compute the region based edge weight in the similar fashion to image intensity, i.e. $w_f((v_p, v_q)) := 1/2||p-q||(g_f(p)+g_f(q))$ where g_f is the edge detection function based on probability values. The internal edge weight is thus the linear combination of the boundary based weight and region based weight: $w_i = w_e + w_f$.

The attraction force imposed by user points is materialized through the interlayer edge weights w_x. We apply distance transform to the user points in each layer of the graph, and the interlayer edge weight is assigned as $w_x = d(v_{pi}, v_{pj})$ where d denotes the distance transform function. This distance weighting produces isolinear bands of weight around the user point, with increasing weight to go through to the next layer as the distance from the user point increases.

Therefore, the energy function for any curve C in our method is a combination of three terms, i.e.

$$\begin{aligned}\mathcal{E}(C, s_1, ..., s_n) = \alpha \sum_{i=1}^{n} ||C(s_i) - X_i|| + \beta \int_0^{L(C)} g(C(s))ds \\ + \int_0^{L(C)} g_f(C(s))ds, \qquad s.t. s_i < s_j, \forall i < j.\end{aligned} \tag{2}$$

The first term is used to enforce the soft constraint by the user points, and it penalizes the path further away from the user points. The second term is the boundary based data term that prefers the path passing through strong edges, whileas the last term is the region based data term which prefers path traveling through abrupt changes in foreground probability. By using the layered graph construction, the minimization of the energy functional is achieved by finding the shortest path from the start point r to the end point t. The Dijkstra's algorithm is used to calculate the shortest path in the layered directed graph. Note, the interlayer edges are unidirectional so that the path can not travel back to previously visited layers.

A smoothing constraint may be added to the energy functional to reduce oscillations of the segmented media-adventitia border. However, for simplicity

we use radial basis function (RBF) interpolation to obtain the final smoothed segmentation. The images are transformed from Cartesian coordinates to Polar coordinates so that the RBF interpolation is reduced to a 1D problem which is efficient to solve.

Table 1. Quantitative comparison. HD: Hausdorff Distance (pixels); AOR: Area Overlap Ratio (%); Spec: Specificity (%); Sens: Sensitivity (%), Acc: Accuracy (%).

Method		HD	AOR	Spec	Sens	Acc
Star Graph-cut	Mean	60.57	81.22	89.22	89.86	89.29
	STD	15.64	1.00	12.00	1.00	6.52
Star Graph-cut with F/B labeling	Mean	43.81	86.05	90.39	93.99	92.17
	STD	23.89	9.00	9.00	5.00	5.65
Proposed method w/o F/B labeling	Mean	46.28	69.34	84.92	89.43	88.12
	STD	9.73	9.24	5.82	10.53	8.76
Proposed method with F/B labeling	Mean	33.57	89.93	94.21	93.14	94.41
	STD	5.35	9.16	3.88	5.37	7.67

3 Experimental Results

The proposed method was evaluated on an IVUS dataset containing 248 manually labeled images from 7 different patients and was compared against the recent star graph-cut method [10] which utilizes user input and a generic shape prior as a constraint. This star shape constraint requires the object boundary does not occlude itself from the center of the object, star point, which is very appropriate for IVUS segmentation. It also allows varies degree of user input, i.e. a single user point (star point) and additional foreground and background labeling. We also show performance of the proposed method with user points alone, i.e. without user strokes.

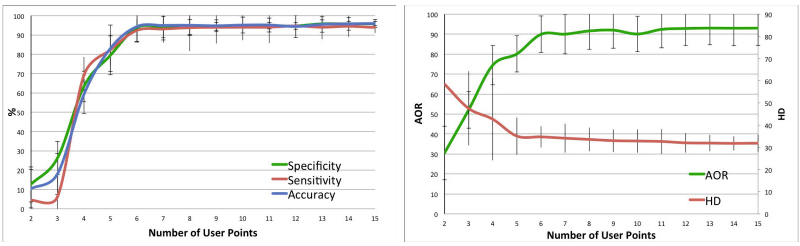

Fig. 3. Initialization dependency test.

The quantitative comparison is based on a number of metrics, including Hausdorff distance, area overlap ratio, specificity, sensitivity and accuracy. Table 1 shows the quantitative results. The star graph-cut method performed reasonably well. However, with foreground and background labeling, the performance clearly

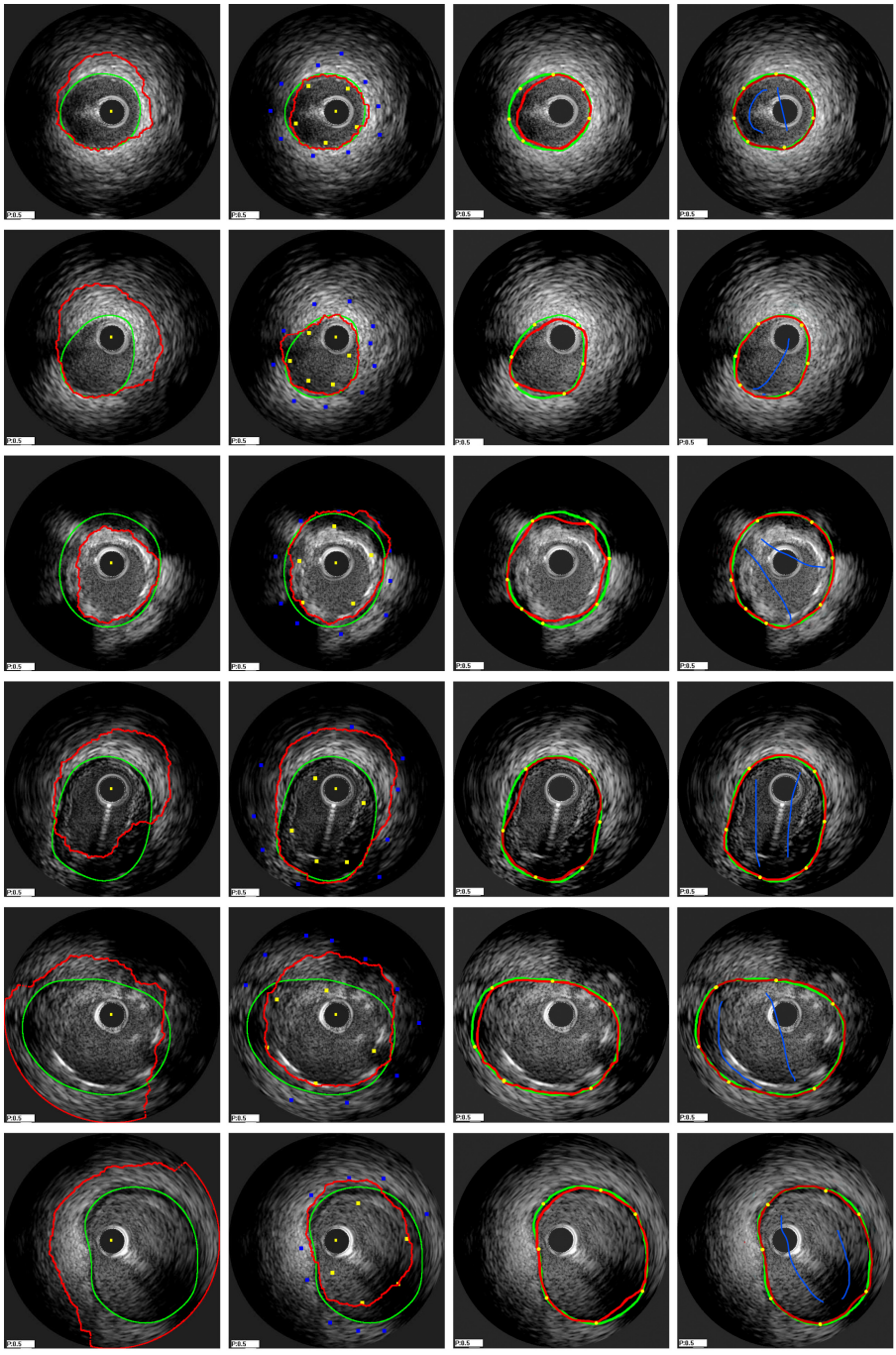

Fig. 4. Comparison between groundtruth (green) and (from left to right) Star Graph Cut [10], Seeded Star Graph Cut, Single Method [13], Proposed Method (red).

improved. The implicit shape prior in star graph construction proved useful in segmenting media-adventitia border which conforms very well to this shape constraint. Comparable performance was achieved for the proposed method without regional support. However, the full proposed method outperformed the rest. Several typical segmentation results are shown in Fig. 4.

To study the robustness of the proposed method, we carried out an initialization dependency test. We tested our method with 15 user points as initialization. We then randomly remove one user point each time for testing until we only have 2 points left for initialization. The overall results using 5 different metrics are shown in Fig. 3. The proposed method achieved good performance with just six user points. Considering in actual application where user input is far experienced than this random process, even less points may be needed.

4 Conclusion

We presented an interactive segmentation technique which combines boundary based and region based object representations. We adopted layered graph representation to simplify computation. The proposed method was compared against a very recent graph cut technique that uses both implicit shape prior and user initialization. Both qualitative and quantitative comparisons on a manually labeled IVUS dataset showed promising performance of the proposed method.

References

1. Katouzian, A., Angelini, E.D., Carlier, S.G., Suri, J.S., Navab, N., Laine, A.F.: A state-of-the-art review on segmentation algorithms in intravascular ultrasound (IVUS) images. IEEE Trans. Info. Tech. in Biomed. 16(5), 823–834 (2012)
2. Luo, Z., Wang, Y., Wang, W.: Estimating coronary artery lumen area with optimization-based contour detection. T-MI 22(4), 564–566 (2003)
3. Katouzian, A., Angelini, E.D., Sturm, B., Laine, A.F.: Automatic detection of luminal borders in ivus images by magnitude-phase histograms of complex brushlet coefficients. In: EMBC, pp. 3072–3076 (2010)
4. Essa, E., Xie, X., Sazonov, I., Nithiarasu, P., Smith, D.: Shape prior model for media-adventitia border segmentation in IVUS using graph cut. In: Menze, B.H., Langs, G., Lu, L., Montillo, A., Tu, Z., Criminisi, A. (eds.) MCV 2012. LNCS, vol. 7766, pp. 114–123. Springer, Heidelberg (2013)
5. Sonka, M., Zhang, X., Siebes, M., Bissing, M.S., DeJong, S.C., Collins, S.M., McKay, C.R.: Segmentation of intravascular ultrasound images: A knowledge-based approach. T-MI 14(4), 719–732 (1995)
6. Brathwaite, P.A., Chandran, K.B., McPherson, D.D., Dove, E.L.: Lumen detection in human IVUS images using region-growing. In: Computers in Cardiology, pp. 37–40 (1996)
7. Boykov, Y., Jolly, M.-P.: Interactive organ segmentation using graph cuts. In: Delp, S.L., DiGoia, A.M., Jaramaz, B. (eds.) MICCAI 2000. LNCS, vol. 1935, pp. 276–286. Springer, Heidelberg (2000)
8. Rother, C., Kolmogorov, V., Blake, A.: Grabcut: interactive foreground extraction using iterated graph cuts. ACM Transactions on Graphics 23(3), 309–314 (2004)

9. Sinop, A.K., Grady, L.: A seeded image segmentation framework unifying graph cuts and random walker which yields a new algorithm. In: ICCV, pp. 1–8 (2007)
10. Veksler, O.: Star shape prior for graph-cut image segmentation. In: Forsyth, D., Torr, P., Zisserman, A. (eds.) ECCV 2008, Part III. LNCS, vol. 5304, pp. 454–467. Springer, Heidelberg (2008)
11. Cohen, L., Kimmel, R.: Global minimum for active contour models: A minimal path approach. IJCV 24(1), 57–78 (1997)
12. Falcáo, A.X., Udupa, J.K., Samarasekera, S., Sharma, S., Hirsch, B.E., de, A., Lotufo, R.: User-steered image segmentation paradigms: Live wire and live lane. Graphical Models and Image Processing 60(4), 233–260 (1998)
13. Windheuser, T., Schoenemann, T., Cremers, D.: Beyond connecting the dots: A polynomial-time algorithm for segmentation and boundary estimation with imprecise user input. In: ICCV, pp. 717–722 (2009)